analytical chemistry

Article

pubs.acs.org/ac

Single-Molecule Measurements of Transient Biomolecular Complexes through Microfluidic Dilution

Mathew H. Horrocks, Luke Rajah, Peter Jönsson, Magnus Kjaergaard, Michele Vendruscolo, Tuomas P. J. Knowles,* and David Klenerman*

Department of Chemistry, University of Cambridge, Cambridge CB2 1EW, U.K.

Supporting Information

ABSTRACT: Single-molecule confocal microscopy experiments require concentrations which are low enough to guarantee that, on average, less than one single molecule resides in the probe volume at any given time. Such concentrations are, however, significantly lower than the dissociation constants of many biological complexes which can therefore dissociate under single-molecule conditions. To address the challenge of observing weakly bound complexes in single-molecule experiments in solution, we have designed a microfluidic device that rapidly dilutes samples by up to one hundred thousand times, allowing the observation of unstable complexes before they dissociate. The device can interface with standard biochemistry laboratory experiments and generates a spatially uniform dilution that is stable over time allowing the quantification of the relative concentrations of different molecular species.

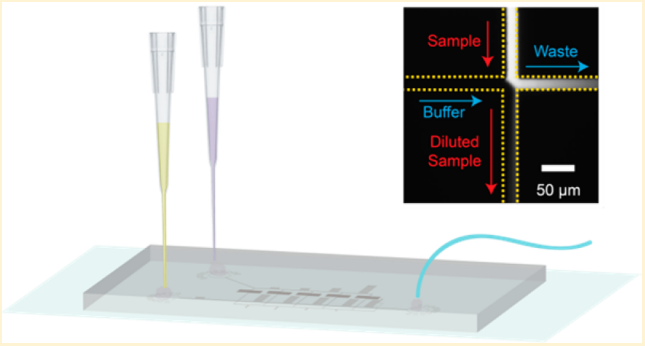

Single-molecule fluorescence spectroscopy is an important tool in the structural analysis of proteins and nucleic acids, as it can resolve subpopulations and characterize rare events by studying fluorophore-tagged molecules one by one. In confocal experiments, single-molecule detection of free-flowing molecules is achieved through a combination of a small confocal probe volume (<1 fL) illuminated by focused laser beams[1] and a low sample concentration, typically less than 100 pM.[2] These two factors ensure that on average there is less than one single molecule in the probe volume. However, picomolar concentrations are significantly below the dissociation constants of most biomolecular complexes, and thus the traditional confocal single-molecule setup is not applicable to the study of unstable complexes.

Several methods for studying these biomolecular complexes with single-molecule fluorescence have been developed. In some cases it is not necessary to label both components in the complex; one partner may be dual-labeled with a Förster resonance energy (FRET) dye pair, and changes in transfer efficiency can be observed after dilution into an excess of unlabeled ligand.[3] However, this is not a general method and requires the ligand to be at a concentration greater than the dissociation constant, which can result in significant background noise from autofluorescence. Wide-field techniques such as total internal reflection fluorescence microscopy (TIRFM) can also be used to study such interactions by immobilizing one biological molecule on the surface and observing binding events with other biological molecules in solution.[4] However, low off-rates are required to study unstable complexes bound to the surface. An alternative strategy for studying biomolecular complexes at low concentrations was developed by Levene et al., who designed a nanostructured device that reduces the effective observation volume to 1 zL (10^{-21} L) allowing for fluorescence correlation spectroscopy (FCS) experiments to be performed at micromolar concentrations.[5] Single-molecule FRET experiments have also been performed on confined molecules within 100 nm nanopipettes, allowing the experiments to be performed at 50-fold higher concentrations than usual,[6] and it may be possible to increase the concentration further if narrower pipettes are used to further reduce the probe volume. However, this would require the use of quartz pipettes increasing the complexity of the experiments substantially, in particular, requiring the alignment of the pipet with the confocal laser probe volume, as well as the prevention of adsorption of molecular species to the surface of the pipet.

Here we present a microfluidic device for the study of unstable complexes, which interfaces with a standard single-molecule fluorescence setup. The microfluidic chip is used to allow a rapid, stable, and automated dilution of the sample down to single-molecule conditions. Since microfluidic chips have become commonplace in single-molecule experiments,[2,7,8] the use of such a device adds no further complexity to the system and is able to combine the benefits of the strategies

Received: April 14, 2013
Accepted: June 19, 2013
Published: June 19, 2013

   dx.doi.org/10.1021/ac4010875 | *Anal. Chem.* 2013, 85, 6855−6859

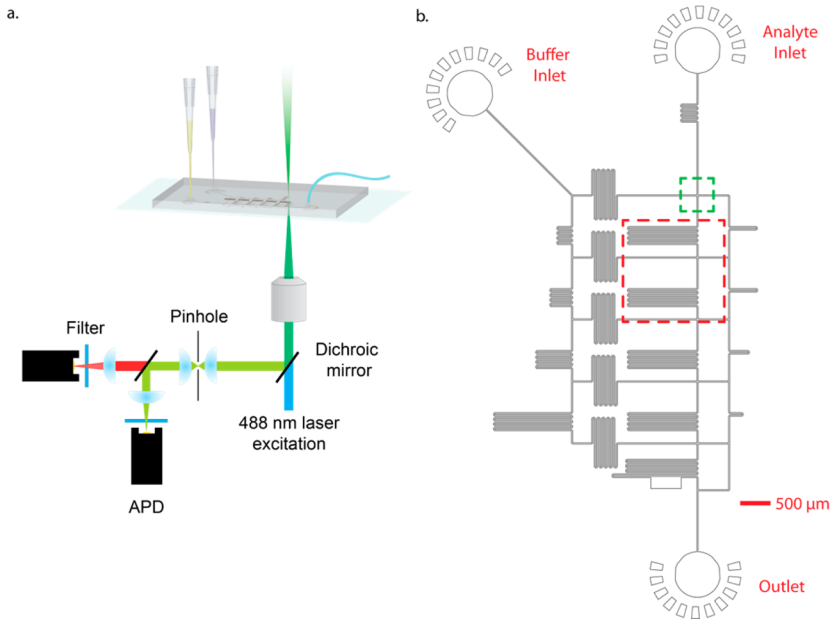

Figure 1. (a) Schematic of the experimental setup, consisting of an inverted confocal fluorescence microscope interfaced with the autodilution device. (b) Plan of the microfluidic device. Each junction between the sample and buffer channel leads to a 1:10 dilution, leading to a 1:100 000 dilution in total. A pressure gradient between the buffer/analyte inlets and the outlet is achieved by withdrawing sample from the outlet. The red and green dashed boxes correspond to the fluorescence images of the regions shown in Figure 2b.

mentioned above for studying unstable complexes with those of the traditional single-molecule setup. In particular, it enables the study of such complexes without any additional surface patterning or surface chemistry modification, and in an automated, continuous, and time-resolved manner.

RESULTS AND DISCUSSION

Figure 1b shows the design of the microfluidic device used to achieve a 1:100 000 dilution. Key to the design of the device is that the flow control is achieved through a single pressure, applied at the outlet, and that changes in the volume of the sample and therefore the hydrostatic pressure are compensated by identical changes in the pressure of the dilution buffer channel, allowing the dilution to be constant over time and space and eliminating the need to insert samples through syringes (see the Supporting Information). At each of the four-way junctions of the device, the sample and the buffer combine at rates which give rise to a 1:10 dilution (Figure 2). There are five four-way junctions in total, leading to an overall dilution of 1:100 000. The lengths of resistor elements within the device, and therefore the relevant flow rates for each dilution step,[9−11] were set using the analogues of Kirchoff's laws for microfluidic circuit design (Supporting Information).

The total dilution factor can be varied by changing the number of dilution steps. The minimum time to allow for 99% mixing of solute with buffer between steps is related to the diffusion coefficient, D (m^2/s), of the species being analyzed and the width of the channel, w, as approximated by eq 1, (for derivation, see the Supporting Information):

$$t_{99\%} \approx \frac{w^2}{2D} \quad (1)$$

If faster dilution times are needed for more unstable complexes, the withdraw rate can be set higher than indicated in eq 1. However, the absolute dilution factor will then be greater than 100 000, as less than 1 in 10 of the molecules will be present in

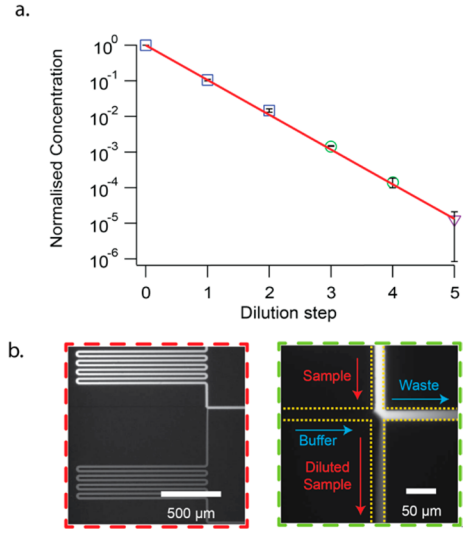

Figure 2. (a) Normalized intensity of fluorescein fluorescence after each step in the dilution device. Each step results in 1:10 dilution, leading to an overall dilution of 1:100 000 after five steps. Blue squares show the normalized concentration determined from a starting solution of 10 mg/mL fluorescein, green circles show the normalized concentration from a starting concentration of 1 mg/mL fluorescein, and the purple triangle shows the concentration determined by comparing the burst rate of the autodilution with that from a manual dilution of 1:100 000. (b) Left: two adjacent dilution stages. Right: the four-way junction at one of the dilution steps (fluorescence image with concentrated fluorescein being diluted), showing clearly that only a small fraction of the solution to be diluted is taken into the next stage.

the fraction progressing to the next dilution stage. Thus, there is a compromise between the accuracy of the dilution factor and the speed of the dilution. For diffusion coefficients typical of biological macromolecules ($D \approx 10^{-6}$ cm^2/s), the total dilution time is on the order of seconds. This makes the device suitable for studying complexes that have an off-rate (k_{off}) lower than

dx.doi.org/10.1021/ac4010875 | Anal. Chem. 2013, 85, 6855−6859

approximately 1 s^{-1}, which is sufficient for most protein−protein and protein−DNA complexes. If the off-rate is higher, and hence only a fraction of molecules are associated, then FRET efficiencies can still be determined, although part of the sample will contribute to the zero-peak. In addition, the width of the channels can be made narrower to decrease the time required for diffusion. We note that the dilution prepared in this manner on chip is uniform in space, a factor which is crucial for the quantification of the relative concentrations of heterogeneous species.

We characterized each step of the dilution using a combination of bulk and single-molecule fluorescence microscopy. Figure 2a shows the mean, normalized fluorescence intensity after each dilution step, demonstrating that each four-way junction results in a 1:10 dilution.

Values for the first four steps were obtained by diluting a fluorescein solution in water from starting concentrations of 1 and 10 mg/mL. Two concentrations were used due to quenching of the fluorophore at high concentration and lack of signal at low concentration. The solution was withdrawn at a flow rate of 5 μL/h, and the fluorescence levels after each stage were measured (mean and SD, n = 3 in different regions). To determine the overall dilution factor, a 2 × 10^{-3} mg/mL solution of fluorescein was first diluted manually by 1:100 000 into PBS before being added to a clean coverslip mounted on the single-molecule confocal microscope (Figure 1a and the Methods section). The sample was illuminated at 488 nm, and light was collected in the green fluorescence channel; bursts with intensity greater than 10 counts/bin were counted, and the burst rate was determined to be 40 ± 10 s^{-1} (mean ± SD, n = 3; the burst rate from buffer alone was 0.16 s^{-1}). The 2 × 10^{-3} mg/mL sample was then diluted using the autodilution device at a withdraw rate of 5 μL/h where the velocity of the molecules in the detection region at this flow rate is dominated by free diffusion. The burst rate in this case, with identical thresholding, was 44 ± 40 s^{-1} (mean ± SD, n = 3 in different devices; the burst rate from buffer alone was 0.15 s^{-1}), matching the manual dilution burst rate within error.

To test the ability to detect weakly associated biological complexes, we designed a DNA duplex with a dissociation rate close to the upper limit of the device. We measured the stability and binding kinetics of the duplex using a combination of thermal melting and stopped-flow spectroscopy, which showed that the DNA duplex had a dissociation constant of 230 nM and an off-rate of 0.129 s^{-1} (see the Supporting Information). One of the strands was labeled with Alexa Fluor 488 (AF488), and the complementary strand was labeled with Alexa Fluor 647 (AF647), and the dye pair was close enough for FRET to occur. A 10 μM concentration of the duplex was first diluted manually by 1:100 000 into PBS before being loaded and passed through the simple one-channel microfluidic device mounted on the single-molecule confocal microscope at a velocity of 0.1 cm s^{-1}. The top panel of Figure 3 shows the FRET efficiency histogram generated. Due to the high off-rate and slow manual dilution, only a zero-peak corresponding to AF488-labeled single-stranded DNA was observed. The 10 μM duplex was then loaded into the autodilution device, with PBS being loaded into the buffer inlet. The device was mounted onto the single-molecule confocal setup, and sample was withdrawn from the device at a rate of 200 μL/h. The mean flow velocity across the dilution channels of the device was measured using fluorescence correlation spectroscopy (FCS) (see the Supporting Information) and was determined to be

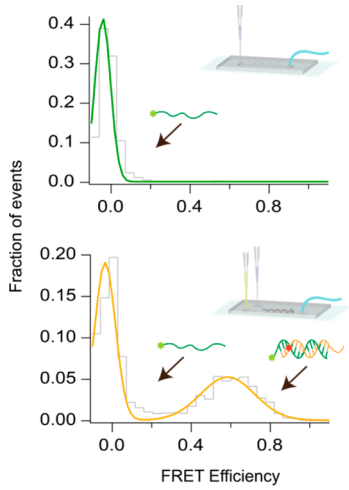

Figure 3. FRET efficiency histograms of the unstable dual labeled DNA duplex with k_{off} = 0.129 s^{-1}. Both data sets were taken at the same flow rate in the detection region (0.1 cm/s) and analyzed using the SUM criterion with a threshold of 15 counts/bin. Top: the manually diluted duplex (10^5× diluted to 10 pM) shows a large zero-peak due to the presence of only single-stranded DNA. Bottom: diluted sample in the autodilution device. Due to the rapid dilution, many events from the double-stranded duplex are observed as a second peak with a higher FRET efficiency. The peaks were fitted to Gaussian distributions using the multipeak fitting package in Igor Pro (Wavemetrics).

1.07 ± 0.02 cm/s, meaning that each dilution step takes approximately 0.93 s, giving a total dilution time of 4.67 s. The typical diffusion coefficient for a 20 base-pair DNA duplex is on the order of 1 × 10^{-10} m^2/s,[12] and so our dilution time is slightly faster than the minimum time of 1.74 s required for the duplex to diffuse across the width of the channel before each dilution step (eq 1). This gives rise to an overall dilution factor of 1:144 000 (using Supporting Information eq 16). The bottom panel of Figure 3 shows the resulting FRET efficiency histogram. As the dilution occurred rapidly, events resulting from the associated DNA duplex were detected (E_{FRET} = 0.6), demonstrating that the device was able to measure FRET efficiency distributions for weakly associated complexes. Typical binned photon-burst data from which the histograms were generated are shown in the Supporting Information (Figure S12).

Although microfluidic devices for on-chip dilution have been designed previously to produce both logarithmic[13,14] and linear dilution series,[15−21] they often require multiple inlet pressures to be controlled (typically using syringe pumps), making them less stable and straightforward to use. More complex implementations of on-chip dilution have also been demonstrated. In one case, an arbitrary dilution factor can be achieved by circulating the solution to be diluted and adding buffer and removing waste during each circuit.[22] However, this requires a complex system of valves in addition to three-layer lithography. This system uses sample volumes as low as 400 nL and requires a minimum mixing time of 22 s. Devices capable of generating a radial concentration gradient have also been designed,[23] as well as chips able to produce gradients in two dimensions with a dilution series over three different components.[24] A simple form of dilution relies on the outward diffusion of a sample into buffer in a flow focusing geometry, forming a distribution which is approximately Gaussian. However, it would be difficult to

dx.doi.org/10.1021/ac4010875 | Anal. Chem. 2013, 85, 6855−6859

achieve stable high dilutions using such a system, since the local concentration of the sample and the flow rate is extremely sensitive to the detector position, which is difficult to place with high precision and can be displaced over the course of a measurement leading to a bias and apparent variability in the concentrations of the species under study.

CONCLUSIONS

Whereas other microfluidic devices have been used to measure the kinetics of protein conformation change after a change in buffer conditions followed by rapid mixing,[7,9,25,26] we have designed a fully automated, easy-to-use, microfluidic device that is able to measure unstable biological complexes under nonequilibrium conditions after high dilution. This device can be used in conjunction with single-molecule confocal microscopy to study biological complexes. Crucially, this implementation requires only a single negative pressure, imposed using a syringe pump, at the outlet of the device. The reagents being drawn into the inlets can thus be maintained in a controlled environment, rather than being discharged from syringes. The use of only one syringe also means that the system is stable at lower flow rates than possible using two or more syringes, since flow rates here are all set relative to a single pressure.

This device will allow a wide range of new biological processes and interactions to be probed at the single-molecule level; for example, for our own work it will allow us to follow protein aggregation reactions in real time and study interactions of chaperones with proteins and ubiquitin chains with substrates.

METHODS

Device Fabrication. Microfluidic channels were fabricated using standard soft-lithography techniques[27] into poly(dimethylsiloxane) (PDMS; Dow Corning) with SU-8 photoresist on silicon masters. The channels were plasma-bonded to glass coverslides (V.W.R., thickness = 1) to create sealed devices. The channel height was 25 μm. Each device was inspected on a white-light microscope (Nikon Ti-U), and only those without dust or aberrations were used.

Synthetic Oligonucleotides. The sequences of the oligonucleotides used in this study are given in Supporting Information Table S2. Oligonucleotides were purchased from ATDBio Ltd. (Southampton, U.K.) and were purified by double HPLC by the supplier. Duplexes were formed by diluting complementary strands into syringe-filtered (pore size 0.02 μm, Whatman, Maidstone, U.K.) phosphate-buffered saline, PBS (0.01 M phosphate buffer, 0.0027 M potassium chloride, and 0.137 M sodium chloride, pH 7.4), heating to 95 °C, and cooling to room temperature over 2 h. Oligo-1 and oligo-2 were combined to form the unstable duplex (K_D = 230 nM, k_{off} = 0.129 s^{-1}) which was used to demonstrate the rapid dilution.

Single-Molecule Measurements. Single-molecule experiments were performed on a custom-built confocal microscope. Briefly, a Gaussian beam at 488 nm (Spectra Physics Cyan CDRH) was directed through the back port of an inverted fluorescence microscope (Nikon Eclipse Ti-U) and reflected by a dichroic mirror through an immersion oil objective (Apochromat 60×, NA 1.40, Nikon) to be focused 10 μm into the detection region of the microfluidic device. Fluorescence was collected via the same objective and reflected by the dichroic mirror and imaged onto a 50 μm pinhole (Thorlabs). A second dichroic mirror (585DRLP Omega Filters) separated the fluorescence into two separate channels. Green fluorescence from Alexa Fluor 488 was first passed through long-pass and band-pass filters (540ALP and 535AF45, Omega Optical Filters) before being focused onto an avalanche photodiode, APD (SPCM-14, Perkin-Elmer, and Waltham, MA). Red fluorescence from Alexa Fluor 647 was also passed through long-pass and band-pass filters (565ALP and 695AF55, Omega Optical Filters) before being focused onto a second APD. Outputs from the two APDs were connected to a custom-programmed field-programmable gate array, FPGA (Colexica), which counted the signals and combined them into time bins (1 ms) which were selected according to the expected residence time of molecules traveling through the confocal volume.[2] A CCD camera (Watek) was used to carefully position the confocal volume within the microfluidic channel. For microfluidic measurements, the device was mounted onto the single-molecule instrument, and data was collected by focusing 10 μm into the center of the device channels. Data was collected for 30 min in all FRET experiments, and the intensity at the back-port of the microscope was 90 μW.

After subtraction of the average autofluorescence for each channel (0.67 counts/bin for the donor channel and 0.541 counts/bin for the acceptor channel), and correction for the spectral cross-talk from the donor channel into the acceptor channel (3%), a threshold of 15 counts/bin (the sum of the photon counts from the donor and acceptor channel) was used to separate the photon-burst events from the dual-labeled DNA duplex from the background. The FRET efficiencies (proximity ratios) are calculated from the measured donor (I_D) and acceptor (I_A) fluorescence intensities according to eq 2:

$$E_{FRET} = \frac{I_A}{I_D + I_A} \quad (2)$$

FRET efficiencies were calculated for all events and combined to form a FRET efficiency histogram.

ASSOCIATED CONTENT

Supporting Information

Device design, modeling of microfluidic flow, determination of thermodynamic parameters for unstable DNA duplex dissociation, measurement of flow rates, and example photon-burst data. This material is available free of charge via the Internet at http://pubs.acs.org.

AUTHOR INFORMATION

Corresponding Author

*E-mail: dk10012@cam.ac.uk (D.K.); tpjk2@cam.ac.uk (T.P.J.K.). Fax: +441223336362.

Author Contributions

The manuscript was written through contributions of all authors. M.H.H. and L.R. contributed equally.

Notes

The authors declare no competing financial interest.

ACKNOWLEDGMENTS

We thank the Biotechnology and Biological Sciences Research Council, the Engineering and Physical Sciences Research Council, and the Frances and Augustus Newman Foundation for financial support. M.H.H. thanks the Royal Society of

Chemistry (Analytical Chemistry Trust Fund) for his studentship. We thank Dr. Rohan T. Ranasinghe for input and useful discussions about this work.

REFERENCES

(1) Cornish, P. V.; Ha, T. *ACS Chem. Biol.* **2007**, *2*, 53−61.
(2) Horrocks, M. H.; Li, H.; Shim, J.-U.; Ranasinghe, R. T.; Clarke, R. W.; Huck, W. T. S.; Abell, C.; Klenerman, D. *Anal. Chem.* **2012**, *84*, 179−185.
(3) Ye, Y.; Blaser, G.; Horrocks, M. H.; Ruedas-Rama, M. J.; Ibrahim, S.; Zhukov, A. A.; Orte, A.; Klenerman, D.; Jackson, S. E.; Komander, D. *Nature* **2012**, *492*, 266−270.
(4) Thompson, N. L.; Axelrod, D. *Biophys. J.* **1983**, *43*, 103−114.
(5) Levene, M. J.; Korlach, J.; Turner, S. W.; Foquet, M.; Craighead, H. G.; Webb, W. W. *Science* **2003**, *299*, 682−686.
(6) Vogelsang, J.; Doose, S.; Sauer, M.; Tinnefeld, P. *Anal. Chem.* **2007**, *79*, 7367−7375.
(7) Gambin, Y.; VanDelinder, V.; Ferreon, A. C. M.; Lemke, E. A.; Groisman, A.; Deniz, A. A. *Nat. Methods* **2011**, *8*, 239−241.
(8) Hofmann, H.; Hillger, F.; Pfeil, S. H.; Hoffmann, A.; Streich, D.; Haenni, D.; Nettels, D.; Lipman, E. A.; Schuler, B. *Proc. Natl. Acad. Sci. U.S.A.* **2010**, *107*, 11793−11798.
(9) Knight, J.; Vishwanath, A.; Brody, J.; Austin, R. *Phys. Rev. Lett.* **1998**, *80*, 3863−3866.
(10) Kim, D.; Chesler, N. C.; Beebe, D. J. *Lab Chip* **2006**, *6*, 639−644.
(11) Bruus, H. *Theoretical Microfluidics*; Oxford University Press: Oxford, U.K., 2007.
(12) Stellwagen, N. C.; Magnusdottir, S.; Gelfi, C.; Righetti, P. G. *Biopolymers* **2001**, *58*, 390−397.
(13) Chen, C.-Y.; Wo, A. M.; Jong, D.-S. *Lab Chip* **2012**, *12*, 794−801.
(14) Hosokawa, M.; Hayashi, T.; Mori, T.; Yoshino, T.; Nakasono, S.; Matsunaga, T. *Anal. Chem.* **2011**, *83*, 3648−3654.
(15) Pihl, J.; Sinclair, J.; Sahlin, E.; Karlsson, M.; Petterson, F.; Olofsson, J.; Orwar, O. *Anal. Chem.* **2005**, *77*, 3897−3903.
(16) Neils, C.; Tyree, Z.; Finlayson, B.; Folch, A. *Lab Chip* **2004**, *4*, 342−350.
(17) Lee, K.; Kim, C.; Kim, Y.; Jung, K.; Ahn, B.; Kang, J. Y.; Oh, K. W. *Biomed. Microdevices* **2010**, *12*, 297−309.
(18) Lee, K.; Kim, C.; Ahn, B.; Panchapakesan, R.; Full, A. R.; Nordee, L.; Kang, J. Y.; Oh, K. W. *Lab Chip* **2009**, *9*, 709−717.
(19) Kim, C.; Lee, K.; Kim, J. H.; Shin, K. S.; Lee, K.-J.; Kim, T. S.; Kang, J. Y. *Lab Chip* **2008**, *8*, 473−479.
(20) Hattori, K.; Sugiura, S.; Kanamori, T. *Lab Chip* **2009**, *9*, 1763−1772.
(21) Yang, M.; Li, C.-W.; Yang, J. *Anal. Chem.* **2002**, *74*, 3991−4001.
(22) Paegel, B. M.; Grover, W. H.; Skelley, A. M.; Mathies, R. A.; Joyce, G. F. *Anal. Chem.* **2006**, *78*, 7522−7527.
(23) Yang, C.-G.; Wu, Y.-F.; Xu, Z.-R.; Wang, J.-H. *Lab Chip* **2011**, *11*, 3305−3312.
(24) Jang, Y.-H.; Hancock, M. J.; Kim, S. B.; Selimović, Š.; Sim, W. Y.; Bae, H.; Khademhosseini, A. *Lab Chip* **2011**, *11*, 3277−3286.
(25) Lipman, E. A.; Schuler, B.; Bakajin, O.; Eaton, W. A. *Science* **2003**, *301*, 1233−1235.
(26) Hertzog, D. E.; Michalet, X.; Jäger, M.; Kong, X.; Santiago, J. G.; Weiss, S.; Bakajin, O. *Anal. Chem.* **2004**, *76*, 7169−7178.
(27) Qin, D.; Xia, Y.; Whitesides, G. M. *Nat. Protoc.* **2010**, *5*, 491−502.